

Statistical anisotropy of CMB as a probe of conformal rolling scenario

S. R. Ramazanov^{a,b*}, G. I. Rubtsov^{b,c†}

^a *Niels Bohr International Academy and Discovery Center, Niels Bohr Institute,
University of Copenhagen, Blegdamsvej 17, DK-2100, Copenhagen, Denmark*

^b *Physics Department, Moscow State University,
Vorobjevy Gory, 119991, Moscow, Russia*

^c *Institute for Nuclear Research of the Russian Academy of Sciences
Prospect of the 60th Anniversary of October 7a, Moscow, Russia, 117312*

May 4, 2012

Abstract

Search for the statistical anisotropy in the CMB data is a powerful tool for constraining models of the early Universe. In this paper we focus on the recently proposed cosmological scenario with conformal rolling. We consider two sub-scenarios, one of which involves a long intermediate stage between conformal rolling and conventional hot epoch. Primordial scalar perturbations generated within these sub-scenarios have different direction-dependent power spectra, both characterized by a single parameter h^2 . We search for the signatures of this anisotropy in the seven-year WMAP data using quadratic maximum likelihood method, first applied for similar purposes by Hanson and Lewis. We confirm the large quadrupole anisotropy detected in V and W bands, which has been argued to originate from systematic effects rather than from cosmology. We construct an estimator for the parameter h^2 . In the case of the sub-scenario with the intermediate stage we set an upper limit $h^2 < 0.045$ at the 95% confidence level. The constraint on h^2 is much weaker in the case of another sub-scenario, where the intermediate stage is absent.

*e-mail: sabir.ra@nbi.dk

†e-mail: grisha@ms2.inr.ac.ru

1 Introduction and summary

Recent advances in the observational cosmology make it real to start probing the most intriguing aspects of the Universe. In particular, it is of importance to inquire whether the statistical isotropy of the scalar perturbations is exact or only approximate. This issue is of special interest because the statistical isotropy is one of the key assumptions of the six-parametric Λ CDM model and is favored by inflation. Thus, the violation of this property in the observed CMB would imply a highly non-trivial extension of the now standard cosmological model. An additional motivation to search for the statistical anisotropy is the possible presence of various anomalies in the CMB data, such as alignment of low multipoles, axis of evil, power asymmetries, cold spots and others [1]–[12].

In the statistically anisotropic but spatially homogeneous Universe, the power spectrum of the primordial scalar perturbations $\zeta(\mathbf{k})$ depends on the direction of the wave vector \mathbf{k} . The power spectrum can then be written as follows,

$$\mathcal{P}_\zeta(\mathbf{k}) = \mathcal{P}_0(k) \left[1 + a(k) \sum_{LM} q_{LM} Y_{LM}(\hat{\mathbf{k}}) \right], \quad (1)$$

where $\hat{\mathbf{k}} = \mathbf{k}/k$. The coefficients q_{LM} parametrize the direction-dependent part, which one expands in spherical harmonics $Y_{LM}(\hat{\mathbf{k}})$. Unlike in Ref. [13], we assume here that the dependence on the wavenumber k may be absorbed into one function $a(k)$. Commutativity of the classical field $\zeta(\mathbf{x})$ yields $\mathcal{P}_\zeta(\mathbf{k}) = \mathcal{P}_\zeta(-\mathbf{k})$ and hence $q_{LM} = 0$ for odd L .

The generic prediction of the inflationary theory is that the power spectrum is isotropic, $a(k) = 0$. However, the statistical anisotropy can be generated in models of inflation involving vector fields [14, 15, 16, 17] or scalar fields with non-minimal kinetic terms [18]; for reviews see also Refs. [19] and [20]. Somewhat more exotic examples are given by introducing Bianchi I geometry [21] or noncommutative field theory [22, 23]. The most common feature of these models is the statistical anisotropy of a special quadrupole type (the only non-vanishing coefficient in a certain reference frame on the celestial sphere is q_{20}). This prediction arises, e.g., in the model with the rotational invariance broken by a space-like vector [14], or in the hybrid inflation incorporating a vector field coupled to the waterfall scalar [15]. However, higher multipoles q_{LM} can also emerge within the inflationary framework, see, e.g., Ref. [18].

In inflationary theory, the observed approximate flatness of the scalar power spectrum is due to the approximate de Sitter symmetry of inflating space-time. It has been suggested some time ago [24] that, alternatively, the flatness of the power spectrum may be a consequence of conformal symmetry. Concrete models of this sort have been proposed in Refs. [25, 26] and further developed in Refs. [27]–[32]. It is this class of models that we focus on in this paper.

In models of Refs. [25, 26] and similar ones, it is assumed that the cosmological evolution starts from or passes through a conformally invariant state with effectively flat geometry.

This state is unstable, and conformal symmetry $SO(4, 2)$ gets broken down to $SO(4, 1)$ by a time-dependent (rolling) scalar field. During this conformal rolling stage, another field of zero conformal weight develops perturbations which automatically have flat power spectrum. These perturbations are reprocessed into adiabatic perturbations by one or another mechanism (e.g., of Refs. [33, 34]) at some later epoch, after the end of conformal rolling. It is then natural that the adiabatic perturbations inherit the properties of the original field perturbations, modulo possible additional non-Gaussianity.

At the conformal rolling stage, the properties of perturbations to both linear and leading non-linear orders are uniquely determined by the underlying conformal symmetry [32], modulo the overall amplitude and a single dimensionless parameter which we call h^2 (in the model of Ref. [25], the amplitude is also determined by h^2 , see Section 2.1). This parameter governs the non-Gaussianity and statistical anisotropy. The statistical anisotropy generated in the conformal rolling scenario is quite different from the predictions of inflation. In particular, the coefficients q_{LM} parametrizing the power spectrum (1) are the random variables rather than fixed parameters of the model.

There are two sub-scenarios of the conformal rolling scenario which differ by the behaviour of the cosmologically interesting modes after the end of the conformal rolling stage. One possibility is that these modes are already superhorizon by the end of conformal rolling and remain frozen until the late hot epoch. The second sub-scenario assumes that there is an intermediate stage at which the field perturbations evolve in a non-trivial way before crossing out the cosmological horizon and getting finally frozen out. In the latter case, the evolution of the field perturbations results in the statistical anisotropy of all even multipoles. Notably, it does not depend on the magnitude of the momentum \mathbf{k} , i.e., $a(k)$ is independent of k [31]. The predictions of the former sub-scenario for the statistical anisotropy are considerably different. To the linear order in the parameter h , one obtains the statistical anisotropy of the general quadrupole type. It is characterized by the amplitude which decreases with the wavenumber k , i.e. $a(k) \propto k^{-1}$ [28]. This means that the corresponding effects in the CMB sky are suppressed at high CMB multipoles l . The statistical anisotropy of the special quadrupole type also appears in the next-to-linear order. Though the effect is suppressed by the additional power of the parameter h , now the amplitude $a(k)$ does not depend on the wavenumber k [28]. Hence, the subleading contribution may make stronger imprint on the CMB.

Signatures of the statistical anisotropy in the CMB temperature maps have been searched for in Refs. [35]–[37]. Motivated by the model of Ref. [14], Groeneboom and Eriksen [35] discovered the evidence for the quadrupole statistical anisotropy in the five-year WMAP data. However, it was found to be nearly aligned with the ecliptic poles. Using quadratic maximum likelihood estimator, Hanson and Lewis [36] extended the analysis to higher multipoles. They also included the relevant prefactor in the covariance neglected in Refs. [14] and [35]. Hanson

and Lewis [36] confirmed the result on the large quadrupole q_{2M} lying nearly in the ecliptic plane. The strongest indication of the statistical isotropy violation, non-zero at the 9σ confidence level, was found in the W band of the five-year WMAP data in Ref. [37]. These findings have been confirmed by the WMAP team [7] in their analysis of the seven-year data. One possible explanation of the anomalous quadrupole is the systematics inherent in the WMAP data. As argued in Ref. [38], large observed statistical anisotropy may result from beam asymmetries rather than have the cosmological origin.

The purpose of this paper is to constrain the parameter h^2 of the conformal rolling scenario from the non-observation of the cosmological statistical anisotropy in the seven-year WMAP data. We follow the general method proposed by Hirata and Seljak for the purpose of studying CMB lensing and known as the quadratic maximum likelihood (QML) estimation [43]. As discussed in Ref. [36], the same idea can be applied to the study of the statistically anisotropic properties of CMB. In this case one assumes that the coefficients q_{LM} are small and expands the log-likelihood of the observed CMB to the second order in these parameters. By maximizing the log-likelihood with respect to the coefficients q_{LM} , one obtains the estimator. Results derived within the QML approximation are in a good agreement with the exact likelihood methods.

We apply this method to construct the estimator for the parameter h^2 . In view of the results quoted, the estimated values are expected to be inconsistent with the statistical isotropy because of the alleged systematics present in the WMAP data. Assuming that the interpretation in terms of systematics is correct, we set the upper limits on the parameter h^2 in the following way. For each value of h^2 , we simulate the parameter sets $\{q_{LM}\}$, and then generate a number of anisotropic maps for each set $\{q_{LM}\}$. From the maps generated, we estimate the values of the parameter h^2 . We require that in 95% cases they should not exceed the value estimated from the observed CMB. In this way we constrain the conformal rolling sub-scenario with the intermediate stage,

$$h^2 < 0.045$$

at the 95% confidence level. The constraint is much weaker in the framework of the alternative sub-scenario. The reason is that the amplitude of the leading order quadrupole decreases as k^{-1} . This translates into the suppression of the statistical anisotropy effects at high CMB multipoles. Thus, the data useful for the analysis are effectively limited, statistical errors are large and the constraint is $h^2 < 190$ at the 95% confidence level. The constraint is improved significantly, once we take into account the subleading contribution to the statistical anisotropy. This contribution is of the special quadrupole type, and has the amplitude $a(k)$, which is independent of the wavenumber k . Thus, the number of CMB multipoles useful in the analysis is much larger. This somewhat compensates the smallness of the constant h ,

and we obtain the stronger constraint,

$$h^2 \ln \frac{H_0}{\Lambda} < 7$$

at the 95% confidence level. Here H_0 is the present value of the Hubble parameter, which plays the role of the ultraviolet cutoff, and Λ is the infrared cutoff. Without going into speculation on the value of the constant Λ , we point out that this constraint is still very weak, in view of the fact that the conformal rolling scenario is self-consistent only at $h^2 \ll 1$ anyway.

We conclude that the statistical anisotropy is the relevant signature of the conformal rolling with the intermediate stage. It is of particular interest in view of the upcoming Planck data. Hopefully, the latter will be free of the quadrupole anomaly. The other expected advantage of the Planck data is the larger range of the CMB multipoles, which translates into smaller statistical errors. These two factors are expected to improve the sensitivity of the data to the parameter h^2 by more than an order of magnitude. On the other hand, statistical anisotropy appears to be a weak signature of the alternative sub-scenario, and the Planck data are not expected to improve the situation significantly. Thus, it makes sense to focus on the other prediction of this sub-scenario, the non-Gaussianity [29, 30]. At the level of bispectrum, the non-Gaussianities in the conformal scenario are not particularly special. The shape of the intrinsic bispectrum is dictated [39] by the symmetry breaking pattern $SO(4, 2) \rightarrow SO(4, 1)$ and coincides with the bispectrum of a spectator massless scalar field in inflationary theory [40, 41] (in fact, the intrinsic bispectrum may vanish for symmetry reasons, see Section 2.1). The non-Gaussianity generated at the conversion epoch is not specific to the conformal scenario either. So, bispectrum alone cannot discriminate between the conformal scenario and, say, inflation equipped with the curvaton mechanism. On the other hand, the non-Gaussianity of a rather peculiar form arises in the trispectrum. Existing constraints (see, e.g. Ref. [42]) are model-dependent and cannot be directly applied to our model. We leave for the future the analysis of the CMB data aiming at the search for the non-Gaussianity characteristic of the conformal scenario.

This paper is organized as follows. In Section 2.1 we review the properties of the field perturbations at the conformal rolling stage. The power spectrum of relevant perturbations generated by the end of their evolution possesses directional dependence. We show this explicitly in Section 2.2. We consider two sub-scenarios: one in which the cosmologically interesting modes are superhorizon by the end of the conformal rolling stage (Section 2.2.1) and another, with long intermediate stage (Section 2.2.2). In Section 3 we review the main ideas of the QML method and construct model-independent estimators for the coefficients q_{LM} . We also construct an estimator for the parameter h^2 . Section 4 contains our main results. We implement the estimators to the seven-year WMAP data and constrain the parameter h^2 of the two sub-scenarios.

2 Conformal rolling scenario

2.1 Fields and their perturbations at conformal rolling

The main ingredient of the conformal rolling scenario [25, 26] is the conformal stage preceding the conventional hot epoch. As we point out below, the properties of the conformal rolling stage are quite general [30, 32], as they are unambiguously determined by conformal symmetry. Yet it is instructive to review a simple explicit model [25] illustrating this scenario. It involves a complex scalar field ϕ , conformally coupled to gravity, which rolls down the negative quartic potential $V(\phi) = -h^2|\phi|^4$, where h is a small parameter. At large field values, the potential is assumed to change and have a minimum at $|\phi| = f_0$ where conformal symmetry is explicitly broken. The field ϕ is a spectator at the conformal rolling stage and somewhat later, i.e., the evolution of the Universe is dominated by some other matter (see Ref. [32] for an alternative version where ϕ is the dominant matter component).

The central object in the model is the phase θ defined by $\phi = |\phi|e^{i\theta}$. Its perturbations $\delta\theta$ start off as vacuum fluctuations and eventually freeze out. By the end of conformal rolling, perturbations $\delta\theta$ have flat power spectrum. Once the radial field $|\phi|$ settles down to f_0 and conformal symmetry gets broken, what remains are the perturbations of the phase, which at this point are isocurvature perturbations. They get reprocessed into adiabatic perturbations at much later epoch. In this way the flat power spectrum of the adiabatic perturbations is obtained. It can be slightly tilted if there is small explicit breaking of conformal symmetry at the conformal rolling stage [27].

Let us discuss conformal rolling in more detail. At this stage, the theory is described by the action

$$S = S_{G+M} + S_\phi ,$$

where S_{G+M} is the action for gravity and some matter that dominates the evolution of the Universe, and

$$S_\phi = \int d^4x \sqrt{-g} \left[g^{\mu\nu} \partial_\mu \phi^* \partial_\nu \phi + \frac{R}{6} \phi^* \phi - V(\phi) \right] \quad (2)$$

is the action for the complex scalar field. Assuming that the background metric is homogeneous, isotropic and spatially flat, one introduces the field $\chi = a\phi$, where a is the scale factor, and obtains its action in conformal coordinates in the Minkowskian form,

$$S[\chi] = \int d^3x d\eta \left(\eta^{\mu\nu} \partial_\mu \chi^* \partial_\nu \chi + h^2 |\chi|^4 \right) .$$

Here $\eta^{\mu\nu}$ is the Minkowski metric and η is the conformal time.

Since the scalar potential is negative, the conformally invariant state $\chi = 0$ is unstable, and the field rolls down its potential. One assumes that the background χ_c is spatially

homogeneous and without loss of generality chooses the background solution real. It is given by

$$\chi_c(\eta) = \frac{1}{h(\eta_\star - \eta)} ,$$

where η_\star is a free parameter, which is interpreted as the end-of-roll time. Let us consider perturbations in this background. To the leading order in h , perturbations $\delta\chi_1 = \sqrt{2}\delta\text{Re}\chi$ and $\delta\chi_2 = \sqrt{2}\text{Im}\chi$ decouple from each other. We begin with the radial perturbations $\delta\chi_1$. They obey the linearized field equation, in momentum representation,

$$(\delta\chi_1)'' + p^2\delta\chi_1 - 6h^2\chi_c^2\delta\chi_1 = 0 .$$

The properly normalized solution is

$$\delta\chi_1 = \frac{1}{4\pi} \sqrt{\frac{\eta_\star - \eta}{2}} H_{5/2}^{(1)}[p(\eta_\star - \eta)] B_{\mathbf{p}} + h.c. ,$$

where $B_{\mathbf{p}}$ and $B_{\mathbf{p}}^\dagger$ are annihilation and creation operators obeying the canonical commutational relations; $H_{5/2}^{(1)}$ is the Hankel function. At late times the solution approaches the asymptotics

$$\delta\chi_1 = \frac{3}{4\pi^{3/2}} \frac{1}{p^{5/2}(\eta_\star - \eta)^2} B_{\mathbf{p}} + h.c. . \quad (3)$$

The behaviour $\delta\chi_1 \sim (\eta_\star - \eta)^{-2}$ is interpreted as a shift of the end-of-roll time η_\star , which now becomes a random field. Indeed, with perturbations included, the radial field $\text{Re}\chi = \chi_c + \delta\chi_1/\sqrt{2}$ can be written at late times as follows

$$\text{Re}\chi = \frac{1}{h[\eta_\star(\mathbf{x}) - \eta]} , \quad (4)$$

where

$$\eta_\star(\mathbf{x}) = \eta_\star + \delta\eta_\star(\mathbf{x}) , \quad (5a)$$

$$\delta\eta_\star(\mathbf{p}) = -\frac{3h}{4\sqrt{2}\pi^{3/2}p^{5/2}} B_{\mathbf{p}} + h.c. . \quad (5b)$$

As it stands, the expression (4) involves all powers of the small parameter h , i.e., it appears to imply some resummation. However, we will be primarily interested in the first non-trivial order in h , so we understand Eq. (4) merely as a convenient book-keeping tool: to the first non-trivial order in h the right hand side of Eq. (4) is equivalent to $\chi_c + \delta\chi_1$. It is natural to assume that the fields are initially in their vacuum state. Then the field $\delta\eta_\star(\mathbf{x})$ is a time-independent Gaussian field with red power spectrum. Clearly, the overall spatially homogeneous shift of the end-of-roll time is irrelevant, since it can be absorbed into the redefinition of η_\star . What is important is the gradient of $\eta_\star(\mathbf{x})$,

$$v_i = -\partial_i\eta_\star(\mathbf{x}) . \quad (6)$$

It has flat power spectrum, while the higher derivatives have blue spectra.

Let us turn to the object of primary interest, namely, the perturbations of the phase θ or, equivalently, perturbations $\delta\chi_2$ of the imaginary part of the field. We are interested in the leading and subleading orders in the small parameter h , so we take the (real) background in the form (4). The linearized field equation for $\delta\chi_2$ reads

$$(\delta\chi_2)'' - \partial_i \partial_i \delta\chi_2 - \frac{2}{[\eta_\star(\mathbf{x}) - \eta]^2} \delta\chi_2 = 0. \quad (7)$$

At early times, when $k(\eta_\star - \eta) \gg 1$, we get back to the Minkowskian massless equation. The solution to Eq. (7) has the following form,

$$\delta\chi_2(\mathbf{x}, \eta) = \int \frac{d^3k}{(2\pi)^{3/2} \sqrt{2k}} (\delta\chi_2^{(-)}(\mathbf{k}, \mathbf{x}, \eta) A_{\mathbf{k}} + h.c.),$$

where $\delta\chi_2^{(-)}(\mathbf{k}, \mathbf{x}, \eta)$ tends to $e^{i\mathbf{k}\mathbf{x} - ik\eta}$ as $\eta \rightarrow -\infty$ and $A_{\mathbf{k}}, A_{\mathbf{k}}^\dagger$ is another set of annihilation and creation operators. Modulo corrections proportional to $\partial_i \partial_j \eta_\star$ and v^2 , the solution with this initial condition is [28]

$$\delta\chi_2^{(-)}(\mathbf{k}, \mathbf{x}, \eta) = -e^{i\mathbf{k}\mathbf{x} - ik\eta_\star(\mathbf{x}) - i\mathbf{k}\mathbf{v}(\eta_\star - \eta)} \sqrt{\frac{\pi}{2} q(\eta_\star(\mathbf{x}) - \eta)} H_{3/2}^{(1)}[q(\eta_\star(\mathbf{x}) - \eta)],$$

where $q = k + \mathbf{k}\mathbf{v}$ and \mathbf{v} is given by Eq. (6). At late times one has $\delta\chi_2 \sim [\eta_\star(\mathbf{x}) - \eta]^{-1}$. As a result, the phase perturbations $\delta\theta = \delta\chi_2/(\sqrt{2}\chi_1)$ freeze out. In this regime, the phase perturbations, including corrections of order $\partial_i \partial_j \eta_\star$ and v^2 , have the following form [28]:

$$\delta\theta(\mathbf{x}, \eta) = \int \frac{d^3k}{\sqrt{k}} \frac{h}{4\pi^{3/2}k} e^{i\gamma^{-1}k_{||}x_{||} + i\mathbf{k}^T \mathbf{x}^T} A_{\mathbf{k}} \left(1 - \frac{\pi}{2k} \frac{k_i k_j}{k^2} \partial_i \partial_j \eta_\star + \frac{\pi}{6k} \partial_i \partial_i \eta_\star \right), \quad (8)$$

where $\gamma = (1 - v^2)^{-1/2}$ is the standard Lorentz factor; $k_{||}$ and \mathbf{k}^T denote the momenta in the direction of the “velocity” \mathbf{v} and in the orthogonal direction, respectively. These are the phase perturbations by the end of conformal rolling. As promised, they do not depend on the conformal time η ,

$$\partial_\eta \delta\theta(\mathbf{x}, \eta)|_{\eta=\eta_\star(\mathbf{x})} = 0. \quad (9)$$

To the leading order in h , the parameter η_\star is independent of \mathbf{x} , so that $\mathbf{v} = 0$, $\partial_i \partial_j \eta_\star = 0$ and the phase perturbations (8) are Gaussian random field with the flat power spectrum and amplitude of order h . To the subleading order, the expression (8) involves another time-independent Gaussian field $\delta\eta_\star$. This leads to both non-Gaussianity and statistical anisotropy of $\delta\theta(\mathbf{x})$ and hence $\zeta(\mathbf{x})$. Note that the symmetry $\theta \rightarrow -\theta$ ensures that the intrinsic bispectrum vanishes in the concrete model we review.

An important remark is in order. Even though we illustrated the conformal rolling mechanism by making use of the concrete model (2), the results are characteristic of the

entire class of conformal models. As an example, the above formulas are valid [30], modulo field redefinition, in the Galilean Genesis model [26] based on conformal Galileon field with higher derivative action [44]. In fact, these formulas hold [32], provided that the theory has the following general properties at the conformal rolling stage: (i) space-time is effectively Minkowskian; (ii) conformal symmetry $SO(4, 2)$ is spontaneously broken down to $SO(4, 1)$ by a homogeneously rolling scalar field of non-zero conformal weight (χ_1 in the above example); (iii) there is another scalar field of zero conformal weight (the phase field θ above) whose perturbations are in the end converted into the adiabatic perturbations. The only qualification is that the latter field need not be compact, so the amplitude of its canonically normalized perturbations can be arbitrary, whereas the overall amplitude of $\delta\theta$ in the model (2) is proportional to the same parameter h that determines the amplitude of the perturbations $\delta\eta_*$ and hence non-linear terms in $\delta\theta$, see Eqs. (5b) and (8).

To avoid confusion, we note that the model (2) is different from the Galilean Genesis model [26] and the pseudo-conformal model of Ref. [32] in that in the latter models, the cosmological background itself is driven by the rolling scalar field (χ_1 in our notations). Therefore, the perturbation of this field (mode $\delta\chi_1$) is gauge-dependent, while the curvature perturbation ζ has blue power spectrum. This, however, does not invalidate the discussion in the previous paragraph. Indeed, the time shift (analogous to our $\delta\eta_*$) can be given a gauge-invariant definition [26]; this field is related to, but different from ζ . Furthermore, at early times, when the conformal mechanism operates in models of Refs. [26, 32], the energy density and pressure of the rolling field are small, so the effects due to gravity are negligible. This is particularly clear in the Newtonian gauge [26, 45], where the metric perturbations are small at early times, while the perturbations in the rolling field have the form equivalent to Eq. (3). In this regime, the curvature perturbation ζ is irrelevant, as long as one is interested in the perturbations of the field similar to our phase θ , and the formulas of this Section remain valid. This has been shown explicitly [45] in the pseudo-conformal model of Ref. [32], both in the Newtonian gauge and in the gauge $\delta\chi_1 = 0$.

2.2 Two sub-scenarios and statistical anisotropy of primordial perturbations

We continue to use the terminology borrowed from the model (2).

At the conformal rolling stage, the phase perturbations $\delta\theta$ get frozen out because of the fast evolving background (4). Once the conformal rolling stage ends and the radial field settles down to a constant value f_0 , the phase becomes a scalar field minimally coupled to gravity. The behavior of its perturbations at later times depends on whether they are super- or subhorizon in the conventional sense by the end of conformal rolling. Accordingly, there are two sub-scenarios which give different predictions for the statistical anisotropy (and

non-Gaussianity as well) [29, 30, 31].

2.2.1 Sub-scenario A

In this sub-scenario, the phase perturbations are already superhorizon by the end of conformal rolling. So, they remain frozen out, and there is a simple relation between the adiabatic and phase perturbations, $\zeta(\mathbf{x}) = \text{const} \cdot \delta\theta(\mathbf{x})$ plus possible non-linear terms, where $\delta\theta(\mathbf{x})$ are the phase perturbations late at the conformal rolling stage. So, the properties of ζ can be read off from Eq. (8), modulo possible non-Gaussianity generated when $\delta\theta$ is converted into ζ .

The interaction of the phase perturbations with the radial ones at the conformal rolling stage leads to non-trivial effects in the spectrum of the primordial perturbations. In particular, it gives rise to the statistical anisotropy. Indeed, let us consider the two-point product $\delta\theta(\mathbf{x})\delta\theta(\mathbf{x}')$ and average it over the realizations of the operators $A_{\mathbf{k}}$ and $A_{\mathbf{k}}^\dagger$. To the leading order, we obtain the flat and isotropic power spectrum. The directional dependence appears once we take into account corrections coming from the derivatives of the end-of-roll time $\eta_*(\mathbf{x})$ and keep only those modes of $\delta\eta_*(\mathbf{x})$ which are still superhorizon today (shorter modes of $\delta\eta_*(\mathbf{x})$ give rise to the non-Gaussianity rather than statistical anisotropy [29, 30]). For so long modes of $\delta\eta_*(\mathbf{x})$, it does not make sense to average over the realizations of the operators $B_{\mathbf{p}}$, $B_{\mathbf{p}}^\dagger$ at this stage. In this way one obtains the power spectrum of the primordial perturbations $\zeta(\mathbf{k})$ [28]:

$$\mathcal{P}_\zeta(\mathbf{k}) = \mathcal{P}_0(k) (1 + Q_1(\mathbf{k}) + Q_2(\mathbf{k})) . \quad (10)$$

The directional dependence is encoded in the functions $Q_1(\mathbf{k})$ and $Q_2(\mathbf{k})$, which originate from the corrections to the linear and next-to-linear orders in the parameter h , respectively,

$$Q_1(\mathbf{k}) = -\frac{\pi}{k} \hat{k}_i \hat{k}_j \left(\partial_i \partial_j \eta_* - \frac{1}{3} \delta_{ij} \partial_k \partial_k \eta_* \right) , \quad (11)$$

$$Q_2(\mathbf{k}) = -\frac{3}{2} (\hat{\mathbf{k}}\mathbf{v})^2 , \quad (12)$$

where $\hat{\mathbf{k}} = \mathbf{k}/k$. First, let us consider the leading order contribution $Q_1(\mathbf{k})$. We expand it in spherical harmonics,

$$Q_1(\mathbf{k}) = a(k) \sum_{LM} q_{LM} Y_{LM}(\hat{\mathbf{k}}) , \quad (13)$$

where

$$a(k) = k^{-1} . \quad (14)$$

By comparing (11) with (13), one concludes that the anisotropic coefficients q_{LM} are Gaussian variables, since they are linearly related to the derivatives of the end-of-roll time $\eta_*(\mathbf{x})$, which

is the Gaussian field. We keep very long modes of $\delta\eta_*(\mathbf{x})$ with $p < H_0$, where H_0 is the present value of the Hubble parameter. At shorter wavelengths the field $\delta\eta_*(\mathbf{x})$ gets averaged out. Therefore, the expression in parenthesis in (11) should be treated as a constant tensor throughout our part of the Universe; retaining its dependence on \mathbf{x} would result in effects suppressed by H_0/k . For this reason, only the quadrupole of the general type survives in Eq. (13). Neither its direction nor precise magnitude can be predicted because of the cosmic variance. Yet its variance in the ensemble of Universes like ours is calculable. One makes use of Eq. (5b) and finds

$$\langle q_{2M} q_{2M'}^* \rangle = \frac{\pi h^2 H_0^2}{25} \delta_{MM'} . \quad (15)$$

For similar reason, the second contribution $Q_2(\mathbf{k})$ also represents the quadrupole statistical anisotropy, but of the special type. It can be expanded in the same fashion as in (13). As compared to the previous case, the amplitude $a(k)$ is independent of the wavenumber k . We will see that this fact is crucial from the viewpoint of the CMB observations. The other important distinction is that the quantities q_{2M} are not Gaussian now. Therefore, it will be convenient to work with the components of the “velocity” \mathbf{v} , which are Gaussian variables with zero means and variances

$$\langle v_i^2 \rangle = \frac{3h^2}{8\pi^2} \ln \frac{H_0}{\Lambda} . \quad (16)$$

Here the present value of the Hubble parameter and the constant Λ appear as the ultraviolet and infrared cutoffs, respectively. The quantities q_{2M} are then given by

$$q_{2M} = -\frac{4\pi v^2}{5} Y_{2M}^*(\hat{\mathbf{v}}) , \quad (17)$$

where $\hat{\mathbf{v}} = \mathbf{v}/v$ is the unit vector in the direction of the “velocity” \mathbf{v} .

Equations (14), (15), (16) and (17) are the starting point of our analysis of the statistical anisotropy in the CMB within the sub-scenario A.

2.2.2 Sub-scenario B

Let us now turn to the second sub-scenario, in which the phase perturbations are still sub-horizon at the end of the conformal rolling stage and exit the cosmological horizon later [31]. This case is rather non-trivial. First, we need to make certain assumptions about the intermediate stage following conformal rolling. Barring fine-tuning, we consider the intermediate stage very long as compared to the interesting cosmological scales, namely,

$$r \equiv k(\eta_1 - \eta_*) \gg 1 , \quad (18)$$

where η_1 is the end-time of the intermediate stage, at which the modes $\delta\theta$ exit the cosmological horizon. In order not to modify the flat power spectrum generated by the end of

conformal rolling, one assumes that the dynamics of the phase perturbations $\delta\theta$ is nearly Minkowskian at the intermediate stage, so that they obey the field equation

$$\partial_\eta^2 \delta\theta - \partial_i \partial_i \delta\theta = 0 . \quad (19)$$

The latter condition appears very restrictive. However, there are at least two cosmological scenarios where it is obeyed. One is the bouncing Universe with the super-stiff equation of state, $p \gg \rho$ [46, 47, 48]; interestingly, cosmological contraction with stiff equation of state is inherent also in the pseudo-conformal Universe model of Ref. [32]. Another is Genesis [26], where the Universe stays static for a very long period of time before it starts to expand rapidly.

Under the above assumptions, the solution to Eq. (19) supplemented with the initial conditions (8) and (9) is given by [31]

$$\delta\theta(\mathbf{x}, \eta_1) = \frac{h}{4\pi^{3/2}} \int \frac{d^3k}{\sqrt{k}} e^{i\mathbf{k}\cdot\mathbf{x}} A_{\mathbf{k}} I + h.c. , \quad (20)$$

where I is the sum of two incoherent waves coming from the direction $\hat{\mathbf{k}}$ and from the opposite direction,

$$I = \frac{1}{2k} \left(e^{i\psi_+} \left[1 - \hat{\mathbf{k}}\mathbf{v}^{(+\hat{\mathbf{k}})} + r(\delta_{ij} - \hat{k}_i \hat{k}_j) \partial_i v_j^{(+\hat{\mathbf{k}})} \right] + e^{i\psi_-} \left(1 - \hat{\mathbf{k}}\mathbf{v}^{(-\hat{\mathbf{k}})} \right) \right) . \quad (21)$$

Here

$$\psi_+ = \psi_+(\mathbf{x}, \hat{\mathbf{k}}) = k\eta_1 - 2k\eta_*(\mathbf{x} + \hat{\mathbf{k}}r), \quad \psi_- = -k\eta_1 ,$$

upper labels $(+\hat{\mathbf{k}})$ and $(-\hat{\mathbf{k}})$ denote quantities calculated at the points $\mathbf{x} + \hat{\mathbf{k}}r$ and $\mathbf{x} - \hat{\mathbf{k}}r$, respectively. Note that Eq. (21) is valid at the horizon exit, so it determines, in fact, the properties of the adiabatic perturbations (again modulo possible additional non-Gaussianity). Note also that under the assumption (18), the modes of $\delta\eta_*$ relevant in Eq. (21) are indeed longer than the size of the visible Universe.

Proceeding as in Section 2.2.1, we arrive at the power spectrum (10), but now with

$$Q(\mathbf{k}) = \hat{k}_i \left(v_i^{(+\hat{\mathbf{k}})} - v_i^{(-\hat{\mathbf{k}})} \right) . \quad (22)$$

In this case all coefficients q_{LM} are generically different from zero. Their variances in an ensemble of Universes are calculated by making use of Eq. (5b) and are given by [31]

$$\langle q_{LM} q_{L'M'}^* \rangle = \frac{3h^2}{\pi} \frac{1}{(L-1)(L+2)} \delta_{LL'} \delta_{MM'} . \quad (23)$$

Notably, the function $a(k)$ does not depend on the momentum, i.e.

$$a(k) = 1 . \quad (24)$$

Equations (23) and (24) determine the statistical anisotropy of the primordial adiabatic perturbations in the sub-scenario B in terms of a single unknown parameter h^2 .

3 Estimators

3.1 Model-independent analysis

Let us first apply the quadratic maximum likelihood (QML) method to construct the estimators for the coefficients q_{LM} . Here we define the latter in a model-independent way, assuming only that the dependence on the wavenumber k can be factorized as in Eq. (1). We closely follow the technique developed in Ref. [36]. In Section 3.2 we use the same ideas when constructing the estimator for the parameter h^2 .

In what follows we use the harmonic representation for the temperature fluctuations and their covariances unless the opposite stated. The log-likelihood of the observed CMB temperature map $\hat{\Theta}$ is given by

$$-\mathcal{L}(\hat{\Theta}|\mathbf{q}) = \frac{1}{2}\hat{\Theta}^\dagger \mathbf{C}^{-1}\hat{\Theta} + \frac{1}{2}\ln \det \mathbf{C} , \quad (25)$$

where \mathbf{q} is the vector of coefficients q_{LM} ; the covariance matrix \mathbf{C} incorporates the theoretical covariance corresponding to the signal as well as the instrumental noise, $\mathbf{C} = \mathbf{S} + \mathbf{N}$. The theoretical covariance is given by

$$S_{lm;l'm'} = \langle \Theta_{lm} \Theta_{l'm'}^* \rangle = i^{l-l'} \frac{2}{\pi} \int d\mathbf{k} \Delta_l(k) \Delta_{l'}(k) P_\zeta(\mathbf{k}) Y_{lm}^*(\hat{\mathbf{k}}) Y_{l'm'}(\hat{\mathbf{k}}) .$$

Here Θ_{lm} are the theoretical temperature fluctuations of the CMB sky $\delta T(\mathbf{n})$ in the harmonic representation,

$$\Theta_{lm} = \int d\Omega \delta T(\mathbf{n}) Y_{lm}^*(\mathbf{n}) ,$$

and $P_\zeta(\mathbf{k})$ is the power spectrum of the primordial perturbations; $\Delta_l(k)$ are transfer functions. Under the assumption of the statistical anisotropy, we write the theoretical covariance as follows,

$$\mathbf{S} = \mathbf{S}^i + \delta\mathbf{S} ,$$

where the leading contribution \mathbf{S}^i comes from the isotropic signal well fitted by the Λ CDM model; the effects of the statistical isotropy violation are incorporated into $\delta\mathbf{S}$. The matrix \mathbf{S}^i is diagonal in the harmonic representation,

$$S_{lm;l'm'}^i = C_l \delta_{ll'} \delta_{mm'} . \quad (26)$$

where C_l is the standard CMB angular spectrum. The matrix $\delta\mathbf{S}$ is given by

$$\delta S_{lm;l'm'} = i^{l'-l} C_{l'} \sum_{LM} q_{LM} \int d\Omega_{\mathbf{k}} Y_{lm}^*(\hat{\mathbf{k}}) Y_{l'm'}(\hat{\mathbf{k}}) Y_{LM}(\hat{\mathbf{k}}) , \quad (27)$$

where

$$C_{ll'} = 4\pi \int d \ln k \Delta_l(k) \Delta_{l'}(k) a(k) \mathcal{P}_\zeta(k) . \quad (28)$$

The integral of three spherical harmonics reads

$$\int d\Omega_{\mathbf{k}} Y_{lm}^*(\hat{\mathbf{k}}) Y_{l'm'}(\hat{\mathbf{k}}) Y_{LM}(\hat{\mathbf{k}}) = (-1)^{m'} G_{ll'}^L C_{lm;l'-m'}^{LM} , \quad (29)$$

where $C_{lm;l',-m'}^{LM}$ are the Clebsch-Gordan coefficients and

$$G_{ll'}^L \equiv \sqrt{\frac{(2l+1)(2l'+1)}{4\pi(2L+1)}} C_{l0l'0}^{L0} .$$

Normally, the estimators for the coefficients q_{LM} are determined by equating the derivative of the log-likelihood to zero,

$$\frac{\partial \mathcal{L}}{\partial \mathbf{q}^\dagger} = 0 .$$

However, the covariance matrix \mathbf{C} is not sparse and direct calculations are too costly. Thus, we need an appropriate approximation to work with. At this point we make use of the QML approach. Assuming that the statistical anisotropy is weak, we expand the log-likelihood derivative to the linear order in \mathbf{q} ,

$$\frac{\partial \mathcal{L}}{\partial \mathbf{q}^\dagger} = \left. \frac{\partial \mathcal{L}}{\partial \mathbf{q}^\dagger} \right|_0 + \left. \frac{\partial^2 \mathcal{L}}{\partial \mathbf{q}^\dagger \partial \mathbf{q}} \right|_0 \mathbf{q} . \quad (30)$$

We replace the second derivative of the log-likelihood in this expansion by its expectation value [36],

$$\left\langle \frac{\partial^2 \mathcal{L}}{\partial \mathbf{q} \partial \mathbf{q}^\dagger} \right\rangle = - \left\langle \frac{\partial \mathcal{L}}{\partial \mathbf{q}} \frac{\partial \mathcal{L}}{\partial \mathbf{q}^\dagger} \right\rangle = -\mathbf{F} , \quad (31)$$

where \mathbf{F} is the Fisher matrix. The first equality in Eq. (31) follows from the normalization condition

$$\int \exp(\mathcal{L}) d\hat{\Theta} = 1 .$$

In what follows we use the derivatives of the log-likelihood calculated under the assumption of the statistical isotropy unless the opposite stated, and omit the subscript “0”. The first derivative of the log-likelihood is then given by

$$\frac{\partial \mathcal{L}}{\partial \mathbf{q}^\dagger} = \frac{1}{2} \hat{\Theta}^\dagger (\mathbf{C}^i)^{-1} \frac{\partial \mathbf{C}}{\partial \mathbf{q}^\dagger} (\mathbf{C}^i)^{-1} \hat{\Theta} - \frac{1}{2} \text{Tr} \left((\mathbf{C}^i)^{-1} \frac{\partial \mathbf{C}}{\partial \mathbf{q}^\dagger} \right) ,$$

where \mathbf{C}^i is the statistically isotropic covariance incorporating the noise, $\mathbf{C}^i = \mathbf{S}^i + \mathbf{N}$. The second term in the right hand side of this equation is, in fact, the average of the first term

over the realizations of CMB. This follows from the identity $\text{Tr}\mathbf{A} = \langle \bar{\mathbf{x}}^\dagger \mathbf{A} \mathbf{C}^{-1} \bar{\mathbf{x}} \rangle$, where \mathbf{A} is any matrix and \mathbf{x} is a vector of Gaussian random variables with the covariance \mathbf{C} . Thus, one writes

$$\frac{\partial \mathcal{L}}{\partial \mathbf{q}^\dagger} = \mathbf{h} - \langle \mathbf{h} \rangle, \quad (32)$$

where

$$\mathbf{h} = \frac{1}{2} \bar{\boldsymbol{\Theta}}^\dagger \frac{\partial \mathbf{C}}{\partial \mathbf{q}^\dagger} \bar{\boldsymbol{\Theta}}, \quad (33)$$

and the quantities $\bar{\boldsymbol{\Theta}}$ are the inverse-variance filtered CMB harmonics calculated in the absence of the statistical anisotropy,

$$\bar{\boldsymbol{\Theta}} = (\mathbf{S}^i + \mathbf{N})^{-1} \hat{\boldsymbol{\Theta}}. \quad (34)$$

By substituting Eqs. (31) and (32) into Eq. (30) and equating the result to zero, we obtain the QML estimator,

$$\mathbf{q} = (\mathbf{F})^{-1} (\mathbf{h} - \langle \mathbf{h} \rangle). \quad (35)$$

In what follows we use the Fisher matrix calculated in the full sky and homogeneous noise approximation [36]. It has only diagonal elements, which do not depend on M ,

$$F_{LM;L'M'} = \delta_{LL'} \delta_{MM'} w \sum_{l,l'} \frac{(2l+1)(2l'+1)}{8\pi} \begin{pmatrix} L & l & l' \\ 0 & 0 & 0 \end{pmatrix}^2 \frac{C_{ll'}^2}{C_l^{\text{tot}} C_{l'}^{\text{tot}}}, \quad (36)$$

where C_l^{tot} is the sum of the standard CMB spectrum C_l and the noise spectrum N_l . The constant w denotes the uncut fraction of the sky. We include this factor to achieve better agreement between the approximate Fisher matrix and the exact one defined as the average over the ensemble of simulated maps with the real sky coverage and inhomogeneous noise.

3.2 Estimator for the parameter h^2

In the framework of the conformal rolling scenario, the coefficients q_{LM} are random variables with zero expectation values. To the linear order in h they are Gaussian and have variances given by Eq. (15) or (23). The variances depend on the constant h^2 , which is the only parameter of the model. This makes it possible to constrain the conformal rolling scenario from the non-observation of the cosmological statistical anisotropy. We again use the QML method to construct the estimator for the parameter h^2 . We do that starting from the Gaussian hypothesis about the coefficients q_{LM} . This hypothesis is particularly appropriate in the context of the sub-scenario B. The non-Gaussian q_{2M} 's appear in the sub-scenario A to the subleading order; we comment on this case in the end of this Section.

The probability density of the coefficients q_{LM} for a given value of h^2 is

$$\mathcal{W}(\mathbf{q}|h^2) \sim \frac{1}{\sqrt{\det \mathbf{Q}}} \exp \left(-\frac{1}{2} \mathbf{q}^\dagger \mathbf{Q}^{-1} \mathbf{q} \right).$$

Here the matrix \mathbf{Q} is the covariance of the anisotropy parameters, $Q_{LM;L'M'} \equiv \langle q_{LM} q_{L'M'}^* \rangle$. To obtain the likelihood of the observed CMB with respect to the parameter h^2 , one integrates the product of two probability densities over the set of the parameters q_{LM} ,

$$\mathcal{W}(\hat{\Theta}|h^2) = \int \mathcal{W}(\hat{\Theta}|\mathbf{q}) \mathcal{W}(\mathbf{q}|h^2) d\mathbf{q} , \quad (37)$$

where $\mathcal{W}(\hat{\Theta}, \mathbf{q}) = \exp[\mathcal{L}(\hat{\Theta}, \mathbf{q})]$ and \mathcal{L} is the log-likelihood introduced in Eq. (25). Following the main idea of the QML estimation, we expand the log-likelihood to the second order in \mathbf{q} ,

$$\mathcal{L} = \mathcal{L}_0 + \frac{\partial \mathcal{L}}{\partial \mathbf{q}} \mathbf{q} - \frac{1}{2} \mathbf{q}^\dagger \mathbf{F} \mathbf{q} ,$$

where we again replaced the second derivative by its expectation value over the CMB isotropic realizations. Now the integral in Eq. (37) takes a simple Gaussian form and can be straightforwardly evaluated,

$$\mathcal{W} \sim \frac{1}{\sqrt{\det(\mathbf{F}\mathbf{Q} + \mathbf{I})}} \exp \left(\frac{1}{2} \frac{\partial \mathcal{L}}{\partial \mathbf{q}^\dagger} (\mathbf{F} + \mathbf{Q}^{-1})^{-1} \frac{\partial \mathcal{L}}{\partial \mathbf{q}} \right) . \quad (38)$$

Maximizing (38) with respect to the parameter h^2 ,

$$\frac{\partial \ln \mathcal{W}(\hat{\Theta}|h^2)}{\partial h^2} = 0 ,$$

we obtain the equation for the estimator of h^2 ,

$$\text{Tr} \left((\mathbf{F}\mathbf{Q} + \mathbf{I})^{-1} \mathbf{F} \frac{\partial \mathbf{Q}}{\partial h^2} \right) = \frac{\partial \mathcal{L}}{\partial \mathbf{q}^\dagger} (\mathbf{F}\mathbf{Q} + \mathbf{I})^{-1} \frac{\partial \mathbf{Q}}{\partial h^2} (\mathbf{F}\mathbf{Q} + \mathbf{I})^{-1} \frac{\partial \mathcal{L}}{\partial \mathbf{q}} .$$

In the full sky and homogeneous noise approximation, the Fisher matrix (36) is diagonal,

$$F_{LM;L'M'} = F_L \delta_{LL'} \delta_{MM'} .$$

The matrix Q has the same property,

$$Q_{LM;L'M'} = \tilde{Q}_L h^2 \delta_{LL'} \delta_{MM'} ,$$

where we introduce the quantities \tilde{Q}_L which do not depend on the parameter h^2 . Then the equation determining the estimator takes the form

$$h^2 \sum_L \frac{(2L+1) F_L^2 \tilde{Q}_L^2}{(1 + F_L \tilde{Q}_L h^2)^2} = \sum_L \frac{(2L+1) F_L \tilde{Q}_L}{(1 + F_L \tilde{Q}_L h^2)^2} (F_L C_L^q - 1) , \quad (39)$$

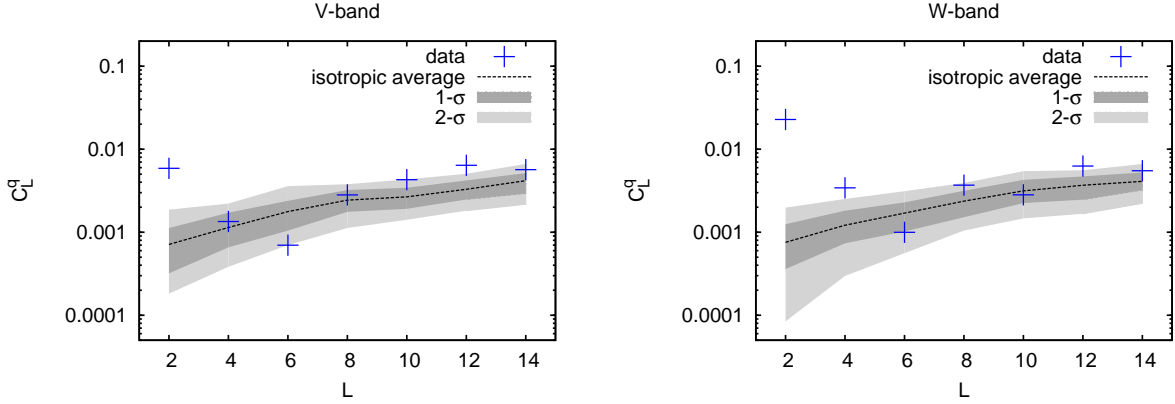


Figure 1: C_L^q of the q_{LM} reconstruction for the V (left) and W (right) bands of the seven-year WMAP data. This analysis assumes $a(k) = 1$ in Eq. (1). The 1σ (dark grey) and 2σ (light grey) confidence intervals are calculated using MC simulated statistically isotropic maps. The analysis is performed with the WMAP temperature analysis mask and $l_{max} = 400$.

where we use the same notation h^2 for the estimator as for the parameter of the model. The quantities C_L^q entering Eq. (39) are given by

$$C_L^q = \frac{1}{2L+1} \sum_M |q_{LM}|^2, \quad (40)$$

where the coefficients q_{LM} are defined by Eq. (35).

Note that it follows from Eq. (39) that if the predicted statistical anisotropy is of the quadrupole form, i.e., with non-zero q_{2M} 's only, then the parameter h^2 can be estimated simply as $h^2 = C_2^q$, modulo obvious additive and multiplicative constants. This is also clear on general grounds. Indeed, the rotational invariance requires that the estimator should be some function of C_2^q , i.e. $h^2 = f(C_2^q)$. In the small statistical anisotropy approximation, we keep only linear terms in the Taylor expansion of the function $f(C_2^q)$. This immediately implies the quoted relationship between h^2 and C_2^q . Since no assumptions about the properties of the random quantities q_{2M} have been used in the latter argument, it holds for non-Gaussian q_{2M} 's, which describe the quadrupole of the special type, see Eq. (17). The only qualification is that the statistical anisotropy is of the order $h^2 \ln \frac{H_0}{\Lambda}$ in that case. Hence, the corresponding estimator reads $h^4 \ln^2 \frac{H_0}{\Lambda} = C_2^q$, up to multiplicative and additive constants.

4 Implementation and results

We search for the statistical anisotropy using WMAP seven-year maps [49, 50]. We study the V and W band data at 61 and 94 GHz. The first step is to implement inverse-variance filtering defined by Eq. (34). We write that equation in the form appropriate for applying the conjugate gradient technique,

$$[(\mathbf{S}^i)^{-1} + \tilde{\mathbf{Y}}^\dagger \mathbf{N}^{-1} \tilde{\mathbf{Y}}] \mathbf{S}^i \bar{\boldsymbol{\Theta}} = \tilde{\mathbf{Y}}^\dagger \mathbf{N}^{-1} \hat{\boldsymbol{\Theta}}. \quad (41)$$

Here we use the pixel representation for the noise covariance \mathbf{N} and the observed CMB temperature $\hat{\boldsymbol{\Theta}}$. The matrix $\tilde{\mathbf{Y}}$ relates the harmonic space covariance and the observed map,

$$\tilde{Y}_{i,lm} = B_l Y_{lm}(\vartheta_i, \varphi_i),$$

where B_l are the beam transfer functions and i labels pixels. We use the foreground reduced V and W seven-year maps [51] provided in HEALPix format [52] with $N_{side} = 512$. For the beam transfer function we use the average of $V1$ and $V2$ functions for V band and the average of $W1$, $W2$, $W3$ and $W4$ for W band.

We consider the noise of the pixels uncorrelated and having the variance σ_0^2/n_{obs} , where σ_0 is 3.137 mK and 6.549 mK for V and W bands, respectively, and n_{obs} is specific to each pixel and tabulated in the maps. To remove foreground contaminated pixels we use the WMAP temperature analysis mask which leaves us with $w = 78\%$ of the sky. We take the noise covariance to be infinite (inverse noise is zero) for masked pixels. The noise model \mathbf{N}^{-1} is constructed using noise covariance and template maps for removing monopole and dipole contributions.

To evaluate the confidence intervals, inverse filtering should be performed on both data and large number of simulated maps. Thus, the system (41) must be well preconditioned. Following Ref. [36], we make use of the multigrid preconditioner, first proposed by Smith et al. in Ref. [54]. It is known to be the fastest to date and has a typical cost of ten minutes when evaluated to $l_{max} = 1000$.

Next, we compute the quantities h_{LM} given by Eq. (33). Using Eqs. (27) and (29), we write them as follows,

$$h_{LM} = \frac{1}{2} \sum_{lm;l'm'} (-1)^{m'} i^{l'-l} \bar{\Theta}_{lm}^* \bar{\Theta}_{l'm'} C_{ll'} G_{ll'}^L C_{lm;l'-m'}^{LM}. \quad (42)$$

We calculate the Clebsch-Gordan coefficients using the GSL [55] and Slatec [56] libraries. The summation in (36) and (42) is performed up to $l_{max} = 400$. We use the publicly available Boltzman code (CAMB) [57] to compute the quantities $C_{ll'}$.

We have simulated large number of statistically isotropic Monte-Carlo (MC) realizations of the field $\hat{\boldsymbol{\Theta}}$ using WMAP noise covariance and beam transfer functions. We store the MC

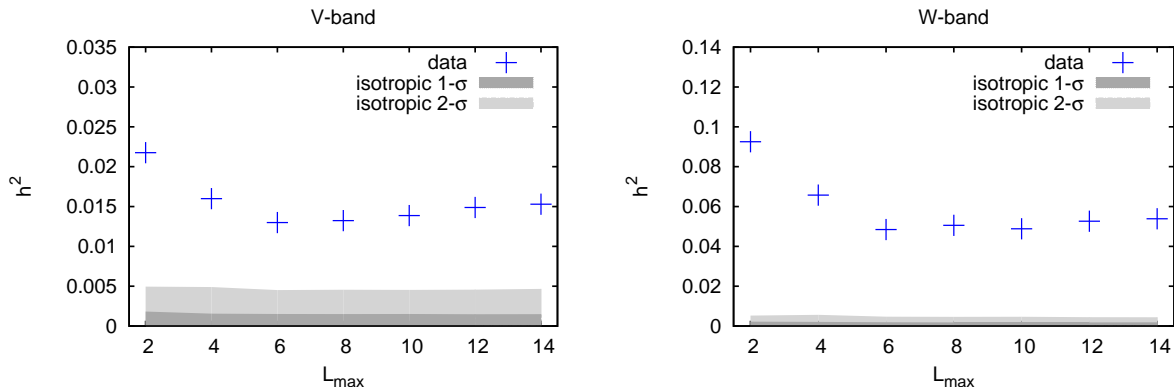


Figure 2: Parameter h^2 of the sub-scenario B reconstructed from the WMAP V band (left) and W band (right). The 1σ (dark grey) and 2σ (light grey) confidence intervals obtained from MC simulations are also shown.

maps in the same format as the original map, and the analysis procedure explained in this Section is applied to both data and MC maps on equal footing.

Now we can check the consistency of the observed CMB with the hypothesis of the statistical isotropy. We begin with the model-independent analysis, as outlined in Section 3.1. We reconstruct coefficients C_L^q , defined by Eq. (40), from the seven-year WMAP data as well as from the MC maps. The results are presented in Fig. 1. They are in a good agreement with the results obtained by Hanson and Lewis [36] for the five-year maps. In particular, we confirm the result on the large quadrupole for the V and W bands. As discussed in Refs. [35]–[37], the preferred quadrupole direction lies very close to the ecliptic poles. Another suspicious thing is the frequency dependence of the signal. Namely, it is non-zero in the W band at much higher confidence level than in the V band. This indicates a systematic effect rather than the cosmological origin. As discussed in Ref. [38], the account of beam asymmetries can provide a complete explanation of the anomaly.

Let us turn to the conformal rolling scenario. First, we consider the version of the model with the intermediate stage (sub-scenario B). The statistical anisotropy is determined by Eqs. (23) and (24). Having the set of the coefficients C_L^q reconstructed from the observed CMB, we solve Eq. (39) and estimate the value of h^2 . We perform the analysis for the multipole numbers starting from $L_{\min} = 2$ and ranging up to $L_{\max} = 2 - 14$. The results are presented in Fig. 2. To evaluate the statistical errors we use about one hundred MC simulated isotropic maps. We see that the isotropic model is ruled out at more than 3σ confidence level even in the V band. However, the large value of h^2 (e.g., $h^2 \approx 0.015$ at $L_{\max} = 14$) is due to the anomalous quadrupole anisotropy, which is argued to have non-cosmological origin.

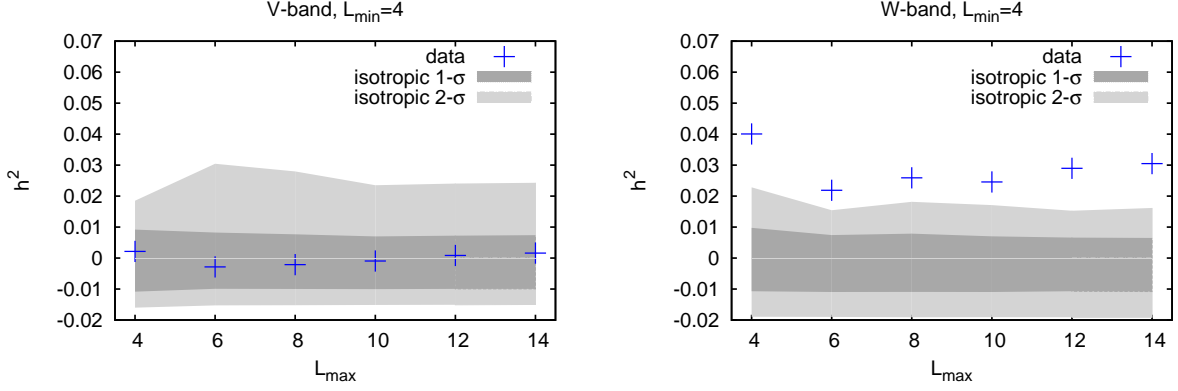


Figure 3: Parameter h^2 of the sub-scenario B reconstructed from higher multipoles ($L_{min} = 4$). Results are plotted for the WMAP V band (left) and W band (right). Shown are the 1σ (dark grey) and 2σ (light grey) confidence intervals obtained from MC simulations.

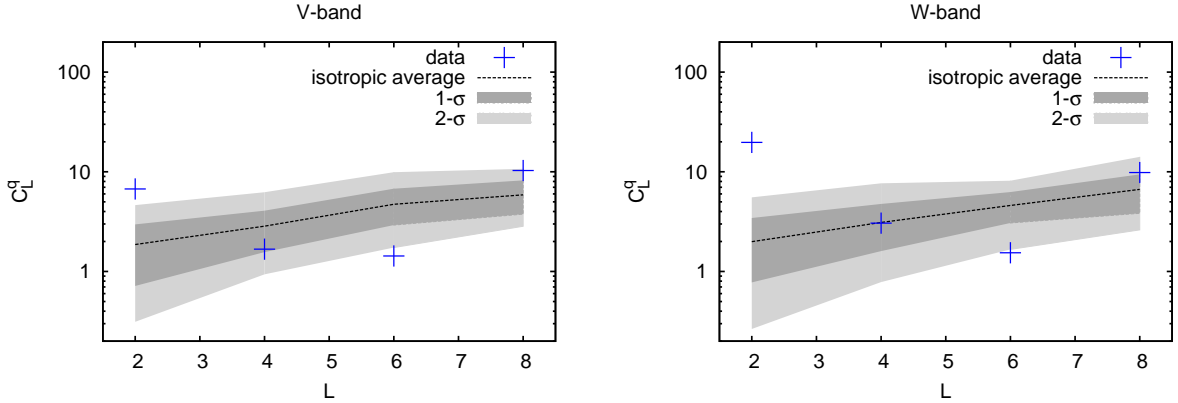


Figure 4: C_L^q of the q_{LM} reconstruction for the V (left) and W (right) bands of the seven-year WMAP. The momentum dependence of the statistical anisotropy is $a(k) = H_0 k^{-1}$. The 1σ (dark grey) and 2σ (light grey) confidence intervals are calculated using MC simulated statistically isotropic maps.

Aiming at constraining the parameter h^2 , we simulate a large number of anisotropic maps for each value of this parameter. We adapt the approach of Ref. [36], and use the following procedure, adequate in the case of small statistical anisotropy.

We first simulate a seed map Θ^i with a covariance \mathbf{S}^i given by Eq. (26). Then we generate a set of coefficients $\{q_{LM}\}$ based on the value of h^2 . The map

$$\Theta^a = \left(\mathbf{I} + \delta \mathbf{S} [\mathbf{S}^i]^{-1} \right)^{1/2} \Theta^i,$$

has covariance $\mathbf{S}^i + \delta\mathbf{S}$, where $\delta\mathbf{S}$ is given by Eq. (27). To the linear order in the anisotropic effects we have

$$\boldsymbol{\Theta}^a = \boldsymbol{\Theta}^i + \frac{1}{2}\delta\mathbf{S}[\mathbf{S}^i]^{-1}\boldsymbol{\Theta}^i.$$

Finally, we multiply the map by the beam transfer function in the harmonic space, convert it to coordinate space and add pixel noise to get statistically anisotropic simulated map $\hat{\boldsymbol{\Theta}}^a$ similar to that observed by WMAP. To set an upper limit, we allow h^2 to be so large that for 95% of simulated anisotropic maps the value of the estimated parameter exceeds the value estimated from the observed CMB map. In this way we obtain the upper limit, which reads

$$h^2 < 0.045 \quad (43)$$

at the 95% confidence level.

In view of the likely non-cosmological origin of the anomalous quadrupole in the statistical anisotropy of the WMAP data, one would like to constrain the parameter h^2 from the non-observation of higher multipoles only. One way to do that would be to follow the same procedure as discussed in Section 3.2 but keep the set $\{q_{2M}\}$ of the quadrupole coefficients fixed and taken from the observational data. In practice, things are simpler. Indeed, the effects of the statistical anisotropy corresponding to different multipole numbers L , M do not interfere with each other, at least in the approximation of small coefficients q_{LM} . To see this, we note that the theoretical reconstruction of the Fisher matrix (36) is diagonal. The covariances of the quantities q_{LM} are diagonal as well. As a consequence, it is straightforward to neglect the effect of the quadrupole modulation by using the estimator for the parameter h^2 as in (39) but with the summation starting from $L_{min} = 4$. The values of h^2 estimated in this way are plotted in Fig. 3. We restrict our analysis to $L_{max} = 14$ and obtain that h^2 is consistent with zero for the V band. Making use of the statistical uncertainty inferred from isotropic MC maps, we obtain the upper limit

$$h^2 < 0.040$$

at the 95% confidence level. Even though omitting the anomalous quadrupole makes the situation cleaner (at least in the V band), this constraint is similar to Eq. (43). The reason is twofold. First, according to Eq. (23), the predicted statistical anisotropy spectrum C_L^q decreases with L as

$$C_L^q \propto \frac{2L+1}{(L-1)(L+2)}.$$

Second, the errors grow with the multipole number roughly as L , see Fig. 1.

With the Planck data available, we expect substantial improvement of the constraint (43). The reason is twofold. Hopefully, the quadrupole anomaly will be absent in the Planck data. Also, the range of the CMB multipoles useful in the analysis will be considerably extended. The error bars, which can be roughly estimated by making use of the inverse Fisher matrix,

scale with the number of multipoles as l_{max}^{-2} . This is clear from the Eq. (36). Taking, e.g., $l_{max} = 1200$, one would be able to reduce the error bars by about an order of magnitude. Hence, the non-observation of the statistical anisotropy will give the constraint as strong as $h^2 \lesssim 0.001$. We conclude that the statistical anisotropy is a promising signature from the viewpoint of the CMB observations in the case of the sub-scenario B.

Finally, we consider the sub-scenario A. To the linear order in constant h , the statistical anisotropy is of the general quadrupole type with decreasing amplitude, $a(k) \propto k^{-1}$. This fact is crucial for the search for the statistical anisotropy in the CMB sky. Indeed, the contribution to the signal $\delta\mathbf{S}$ is additionally suppressed by the CMB multipole number l . This suppression is due to the fact that the integral in Eq. (28) is saturated, roughly speaking, at $k \sim lH_0$. Effectively, it results in low statistics of the relevant CMB multipoles and large statistical errors, which severely restrict the opportunity to observe the (cosmological) statistical anisotropy of the type predicted. Somewhat loosely we apply the QML estimator to the seven-year WMAP data. In Fig. 4 we show the results for C_L^q of the WMAP reconstructed coefficients q_{LM} , assuming $a(k) = H_0 k^{-1}$, but not restricting yet to the quadrupole-only q_{LM} . We apply the procedure used in the case of the sub-scenario with the intermediate stage, to constrain the sub-scenario A; to this end, the quadrupole point $L = 2$ in Fig. 4 is relevant only. The limit on the parameter h^2 then reads

$$h^2 < 190$$

at the 95% confidence level. Note, however, that for large values of h^2 , the QML procedure is questionable. This limit can be viewed merely as an indication that the leading order contribution to the statistical anisotropy is in fact negligible. The stronger constraint comes from the subleading contribution encoded in (12). The reason is that the amplitude $a(k)$ is independent of the wavenumber k in this case. Thus, the suppression at high CMB multipoles is absent, and the range of relevant l 's is extended up to $l_{max} = 400$. Since the quantities q_{2M} are non-Gaussian in this particular case, the constraining procedure is somewhat different. First, we generate the components of the “velocity” \mathbf{v} starting from a given value of the effective constant $h^2 \ln \frac{H_0}{\Lambda}$. Then, using (17), we calculate the coefficients q_{2M} . The quantity $C_2^q = \frac{1}{5} \sum_M |q_{2M}|^2$ constructed out of these q_{2M} is compared with the one estimated from the seven-year WMAP data. In this way we obtain the constraint, which reads

$$h^2 \ln \frac{H_0}{\Lambda} < 7 \quad (44)$$

at the 95% confidence level. Assuming that the logarithmic enhancement is not particularly strong, we conclude that this constraint is still weak. Note also that the statistical anisotropy predicted by the sub-scenario A is of the same type as in some inflationary models [14] – [17]. Thus, it cannot be used to discriminate our model from other models of the generation of primordial perturbations. Fortunately, the sub-scenario A gives rise to the non-Gaussianity

in the trispectrum [29, 30], which is in the sharp contrast with the inflationary predictions. We leave for the future search for the corresponding signatures in the CMB sky.

Acknowledgements

We are indebted to V. Rubakov for numerous helpful suggestions at all stages. We are grateful to D. Hanson for kindly providing the code for inverse variance filtering. We would like to thank A. Lewis, P. Naselsky, M. Sazhin and O. Verkhodanov for fruitful discussions. The work is supported in part by the RFBR grants 11-02-01528a and 12-02-00653a (GR), by the grants of the President of the Russian Federation NS-5590.2012.2, MK-1632.2011.2 (GR), by the grant of the Government of Russian Federation 11.G34.31.0047 (GR). The numerical part of the work has been done at the cluster of the Theoretical Division of INR RAS.

References

- [1] M. Tegmark, A. de Oliveira-Costa and A. Hamilton, Phys. Rev. D **68** (2003) 123523 [arXiv:astro-ph/0302496].
- [2] P. Bielewicz, H. K. Eriksen, A. J. Banday, K. M. Gorski and P. B. Lilje, Astrophys. J. **635** (2005) 750 [arXiv:astro-ph/0507186].
- [3] C. J. Copi, D. Huterer, D. J. Schwarz and G. D. Starkman, Mon. Not. Roy. Astron. Soc. **367** (2006) 79 [arXiv:astro-ph/0508047].
- [4] K. Land and J. Magueijo, Phys. Rev. Lett. **95** (2005) 071301 [arXiv:astro-ph/0502237].
- [5] F. K. Hansen, A. J. Banday, K. M. Gorski, H. K. Eriksen and P. B. Lilje, Astrophys. J. **704** (2009) 1448 [arXiv:0812.3795 [astro-ph]].
- [6] H. K. Eriksen, F. K. Hansen, A. J. Banday, K. M. Gorski, and P. B. Lilje, Astrophys. J. **605**, 14 (2004), [arXiv:0307507 [astro-ph]].
- [7] C. L. Bennett, R. S. Hill, G. Hinshaw, D. Larson, K. M. Smith, J. Dunkley, B. Gold and M. Halpern *et al.*, Astrophys. J. Suppl. **192**, 17 (2011) [arXiv:1001.4758 [astro-ph.CO]].
- [8] M. Cruz, L. Cayon, E. Martinez-Gonzalez, P. Vielva and J. Jin, Astrophys. J. **655** (2007) 11 [arXiv:astro-ph/0603859].
- [9] O.V. Verkhodanov, to appear in Physics Uspekhi.

- [10] J. Kim and P. Naselsky, *Astrophys. J.* **714** (2010) L265 [arXiv:1001.4613 [astro-ph.CO]].
- [11] J. Kim and P. Naselsky, *Phys. Rev. D* **82** (2010) 063002 [arXiv:1002.0148 [astro-ph.CO]].
- [12] C. Rath, P. Schuecker and A. J. Banday, *Phys. Rev. Lett.* **102** (2009) 131301 [arXiv:astro-ph/0702163].
- [13] A. R. Pullen and M. Kamionkowski, *Phys. Rev. D* **76** (2007) 103529 [arXiv:0709.1144 [astro-ph]].
- [14] L. Ackerman, S. M. Carroll and M. B. Wise, *Phys. Rev. D* **75** (2007) 083502 [Erratum-*ibid.* **80** (2009) 069901] [arXiv:astro-ph/0701357].
- [15] S. Yokoyama and J. Soda, *JCAP* **0808** (2008) 005 [arXiv:0805.4265 [astro-ph]].
- [16] K. Dimopoulos, M. Karčiauskas, D. H. Lyth and Y. Rodriguez, *JCAP* **0905** (2009) 013 [arXiv:0809.1055 [astro-ph]].
- [17] K. Dimopoulos, M. Karčiauskas and J. M. Wagstaff, *Phys. Lett. B* **683** (2010) 298 [arXiv:0909.0475 [hep-ph]].
- [18] C. Armendariz-Picon, *JCAP* **0603** (2006) 002 [arXiv:astro-ph/0509893].
- [19] K. Dimopoulos, arXiv:1107.2779 [hep-ph].
- [20] J. Soda, arXiv:1201.6434 [hep-th].
- [21] A. E. Gumrukcuoglu, C. R. Contaldi and M. Peloso, *JCAP* **0711** (2007) 005 [arXiv:0707.4179 [astro-ph]].
- [22] E. Akofer, A. P. Balachandran, S. G. Jo, A. Joseph and B. A. Qureshi, “Direction-Dependent CMB Power Spectrum and Statistical Anisotropy from Noncommutative Geometry,” *JHEP* **0805**, 092 (2008) [arXiv:0710.5897 [astro-ph]].
- [23] T. S. Koivisto and D. F. Mota, *JHEP* **1102** (2011) 061 [arXiv:1011.2126 [astro-ph.CO]].
- [24] I. Antoniadis, P. O. Mazur and E. Mottola, *Phys. Rev. Lett.* **79** (1997) 14 [arXiv:astro-ph/9611208].
- [25] V. A. Rubakov, *JCAP* **0909** (2009) 030 [arXiv:0906.3693 [hep-th]].
- [26] P. Creminelli, A. Nicolis and E. Trincherini, *JCAP* **1011** (2010) 021 [arXiv:1007.0027 [hep-th]].
- [27] M. Osipov and V. Rubakov, *JETP Lett.* **93** (2011) 52 [arXiv:1007.3417 [hep-th]].

- [28] M. Libanov and V. Rubakov, JCAP **1011** (2010) 045 [arXiv:1007.4949 [hep-th]].
- [29] M. Libanov, S. Mironov and V. Rubakov, Prog. Theor. Phys. Suppl. **190** (2011) 120 [arXiv:1012.5737 [hep-th]].
- [30] M. Libanov, S. Mironov and V. Rubakov, Phys. Rev. D **84** (2011) 083502 [arXiv:1105.6230 [astro-ph.CO]].
- [31] M. Libanov, S. Ramazanov and V. Rubakov, JCAP **1106** (2011) 010 [arXiv:1102.1390 [hep-th]].
- [32] K. Hinterbichler and J. Khoury, arXiv:1106.1428 [hep-th].
- [33] S. Mollerach, Phys. Rev. D **42**, 313 (1990);
A. D. Linde and V. F. Mukhanov, Phys. Rev. D **56** (1997), 535 [arXiv:9610219 [astro-ph]];
K. Enqvist and M. S. Sloth, Nucl. Phys. B **626** (2002), 395 [arXiv:0109214 [hep-ph]];
D. H. Lyth and D. Wands, Phys. Lett. B **524** (2002), 5 [arXiv:0110002 [hep-ph]];
T. Moroi and T. Takahashi, Phys. Lett. B **522** (2001), 215 [Erratum-ibid. B **539** (2002), 303] [arXiv:0110096 [hep-ph]];
K. Dimopoulos, D. H. Lyth, A. Notari and A. Riotto, JHEP **0307**, (2003), 053 [arXiv:0304050 [hep-ph]].
- [34] G. Dvali, A. Gruzinov and M. Zaldarriaga, Phys. Rev. D **69** (2004), 023505 [arXiv:0303591 [astro-ph]];
L. Kofman, [arXiv:0303614 [astro-ph]];
G. Dvali, A. Gruzinov and M. Zaldarriaga, Phys. Rev. D **69** (2004), 083505 [arXiv:0305548 [astro-ph]].
- [35] N. E. Groeneboom and H. K. Eriksen, Astrophys. J. **690** (2009) 1807 [arXiv:0807.2242 [astro-ph]].
- [36] D. Hanson and A. Lewis, Phys. Rev. D **80** (2009) 063004 [arXiv:0908.0963 [astro-ph.CO]].
- [37] N. E. Groeneboom, L. Ackerman, I. K. Wehus and H. K. Eriksen, Astrophys. J. **722** (2010) 452 [arXiv:0911.0150 [astro-ph.CO]].
- [38] D. Hanson, A. Lewis and A. Challinor, Phys. Rev. D **81** (2010) 103003 [arXiv:1003.0198 [astro-ph.CO]].
- [39] K. Hinterbichler, A. Joyce and J. Khoury, arXiv:1202.6056 [hep-th].

- [40] M. Zaldarriaga, Phys. Rev. D **69** (2004) 043508 [astro-ph/0306006].
- [41] P. Creminelli, Phys. Rev. D **85** (2012) 041302 [arXiv:1108.0874 [hep-th]].
- [42] J. R. Fergusson, D. M. Regan and E. P. S. Shellard, arXiv:1012.6039 [astro-ph.CO].
- [43] C. M. Hirata and U. Seljak, Phys. Rev. D **67** (2003) 043001 [arXiv:astro-ph/0209489].
- [44] A. Nicolis, R. Rattazzi and E. Trincherini, Phys. Rev. D **79** (2009) 064036 [arXiv:0811.2197 [hep-th]].
- [45] M. Libanov and V. Rubakov, arXiv:1107.1036 [hep-th].
- [46] J. K. Erickson, D. H. Wesley, P. J. Steinhardt and N. Turok, Phys. Rev. D **69** (2004) 063514; [arXiv:0312009 [hep-th]].
D. Garfinkle, W. C. Lim, F. Pretorius and P. J. Steinhardt, Phys. Rev. D **78** (2008) 083537; [arXiv:0808.0542 [hep-th]].
- [47] E. I. Buchbinder, J. Khoury and B. A. Ovrut, Phys. Rev. D **76** (2007) 123503; [arXiv:0702154 [hep-th]].
P. Creminelli and L. Senatore, JCAP **0711** (2007) 010; [arXiv:0702165 [hep-th]].
- [48] J. L. Lehnert, Phys. Rept. **465** (2008) 223; [arXiv:0806.1245 [astro-ph]].
- [49] N. Jarosik, C. L. Bennett, J. Dunkley, B. Gold, M. R. Greason, M. Halpern, R. S. Hill and G. Hinshaw *et al.*, Astrophys. J. Suppl. **192**, 14 (2011) [arXiv:1001.4744 [astro-ph.CO]].
- [50] E. Komatsu *et al.* [WMAP Collaboration], Astrophys. J. Suppl. **192**, 18 (2011) [arXiv:1001.4538 [astro-ph.CO]].
- [51] <http://lambda.gsfc.nasa.gov/>
- [52] K. M. Gorski, E. Hivon, A. J. Banday, B. D. Wandelt, F. K. Hansen, M. Reinecke and M. Bartelman, Astrophys. J. **622**, 759 (2005) [arXiv:0409513 [astro-ph]].
- [53] S. P. Oh, D. N. Spergel, and G. Hinshaw, Astrophys. J. **510**, 551 (1999), [arXiv:9805339 [astro-ph]].
- [54] K. M. Smith, O. Zahn, and O. Dore, Phys. Rev. D **76**, 043510 (2007), [arXiv:0705.3980 [astro-ph]].
- [55] <http://www.gnu.org/software/gsl/>
- [56] <http://www.netlib.org/slatec/>

- [57] A. Lewis, A. Challinor and A. Lasenby, *Astrophys. J.* **538** (2000) 473 [arXiv:astro-ph/9911177].